Crystal structure of asHPAL as a useful aldolase for the two-step stereoselective synthesis of 4-hydroxyisoleucine : understanding the reaction mechanism and expanding the substrate specificity

博士論文（要約）

Crystal structure of asHPAL as a useful aldolase for the two-step stereoselective synthesis of 4-hydroxyisoleucine: understanding the reaction mechanism and expanding the substrate specificity

（4-Hydroxyisoleucine合成に関わる酵素asHPALのX線結晶構造解析と基質選択性の拡大）

GUO LINJUN

郭 琳 珺

Contents

Abbreviations

4-HIL	4-hydroxyisoleucine
asHPAL	4-hydroxy-3-methyl-2-keto-pentanoate aldolase from *Arthrobacter simplex* strain AKU 626
BCAT	branched-chain aminotransferase
Bis-tris	bis(2-hydroxyethyl)-iminotris(hydroxymethyl)methane
BLAST	Basic Local Alignment Search Tool
CBB R-250	Coomassie Brilliant Blue R-250
DDS-d_6	3-(trimethylsilyl)-1-propane-1,1,2,2,3,3-d_6-sulfonate
DNA	deoxyribonucleic acid
DTT	dithiothreitol
ESI-TOF-MS	electrospray ionization time-of-flight mass spectrometry
GITC	2,3,4,6-tetra-*O*-acetyl-β-D-glucopyranosyl isothiocyanate
HEPES	4-(2-hydroxyethyl)-1-piperazineethanesulfonic acid
HMKP	4-hydroxy-3-methyl-2-keto-pentanoate
HPLC	high performance liquid chromatography
IPTG	isopropyl β-D-1-thiogalactopyranoside
LB	Luria-Bertani
PCR	polymerase chain reaction
PDB	protein data bank
PEG	polyethylene glycol
PF	Photon Factory
PLP	pyridoxal phosphate
RMSD	root-mean-square deviation

SDS-PAGE	sodium dodecyl sulfate-polyacrylamide gel electrophoresis
TIM	triosephosphate isomerase
Tris	*tris*(hydroxymethyl)aminomethane

Chapter 1

Introduction

1.1 Chirality and chiral synthesis

Chirality is the configuration, or handedness (left or right), of a molecule that cannot be completely overlapped by its enantiomer (mirror image of the molecule). Chirality is common in organic molecules due to the presence of asymmetric carbon atoms [1]. At present, more than 60% of commercially available drugs are sold as single enantiomers [2, 3].

It is generally understood that different configurations of a given molecule often possess different properties. The enantiomer of vitamin C, which shows no pharmacological activity, cannot be absorbed by humans when ingested [4]. Quinidine and its stereoisomer quinine possess both anti-malarial and myocardial depressive properties. Quinidine is also used as an anti-arrhythmic drug [5]. Thalidomide is an immunomodulatory drug that is used for nausea and for alleviating morning sickness in pregnant women. This drug is functional only in *R*-form, whereas its *S*-form has been reported to be strongly teratogenic and is estimated to have caused phocomelia in ten thousand infants [6]. The ability to obtain a single enantiomer therefore significantly impacts not only drug efficacy but also drug safety.

There are three well-known approaches used to produce a single enantiomer of interest: chiral resolution to separate a desired single enantiomer from a racemic mixture (a mixture with equal parts left- and right-handed enantiomers of a chiral molecule) [7]; the chiral switch method to transform the racemic mixture into a single enantiomer [7]; and the chiral synthesis method, which involves either a single reaction or a chain of reactions, to generate one or more new elements of chirality and obtain the target enantiomer directly [8]. With chiral resolution, only 50% of the target enantiomer is obtained. The chiral switch is required for an additional transformation reaction after synthesis. Compared with these methods, the chiral synthesis method is more economical in terms of material and energy due to a lower workload. These two advantages make the method more valued, and thus, this method is widely applied in

chemical industries [1].

The chiral synthesis methods proposed thus far are divided into chemical synthesis methods and biocatalysis methods. Chemical synthesis methods include the following: enantioselective catalysis using chiral coordination complexes [9, 10]; stereoselective catalysis using chiral auxiliaries, which are combined with a prochiral substrate to form an intermediate that controls the stereoselectivity of a subsequent reaction to generate a chiral product [11]; and chiral pool synthesis, which directly connects an available chiral starting compound with another compound to generate a new chiral compound. The biocatalysis method uses enzymes to synthesize the target enantiomer preferentially [8]. Organic solvent and heavy metals are widely used in the chemical synthesis methods. In contrast, the biocatalysis method is more commonly used in industry when it demonstrates the advantages of considerably high stereoselectivity, relatively mild reaction conditions, and a less harmful impact on human environment [12].

1.2 Aldol reaction

An aldol is a compound with β-hydroxyl and carbonyl groups and is a common structural unit that can be found in many important compounds [13], such as the cholesterol-lowering drug atorvastatin and the immunosuppressive drug tacrolimus. Aldols can be generated by the aldol reaction of two reacting carbonyl compounds [1, 14-17]. This reaction is particularly useful because it can generate new chiral centers (one or more) and form a new carbon-carbon bond in a single reaction [18, 19]. The reaction mechanism and stereoselectivity have been improved through extensive studies [20-24]. There are many methodologies that promote aldol reactions in high yield and control the relative and absolute stereochemical configurations at

chiral centers simultaneously. The enantioselective regulation can be achieved by the use of metal ions [25], specific electrophiles [26], enzymes as biocatalysts [15, 16], etc.

The aldol reaction proceeds by two fundamentally different mechanisms (Fig 1-1) [15, 16]. One of the reaction mechanisms includes an enol formation step (Fig. 1-1A). Carbonyl compounds with one or two α-carbons (aldehyde and ketone) are generally nucleophilic at the α-carbon and thus can be converted to enol intermediates in acidic conditions. The intermediate attacks the protonated carbonyl carbon of aldehyde to generate an aldol. The other reaction mechanism is via an enolate intermediate, which is formed by deprotonation at the α-carbon of the carbonyl compound and then attacks the electrophile of aldehyde to generate aldol (Fig. 1-1B).

1.3 Aldolases

Aldolases are a type of enzyme that can catalyze the aldol reaction for specific substrates. The reaction catalyzed by aldolases can proceed under mild conditions and thus has the advantage of low environmental impact. In addition, some aldolases have the potential to be used as biocatalysts for stereoselective aldol reactions. Aldolases are divided into two classes (I and II) according to activation states of their reaction processes [27]. The reaction mechanism of aldolases has been reported and thoroughly discussed [28-30]. Class I aldolases form a ketimine Schiff base intermediate with the substrate using a lysine residue at the active site [31, 32]. Class II aldolases form an enolate intermediate from the substrate using metal ions that polarize the carbonyl group of the substrates [33]. Aldolases are further classified into more than 30 subfamilies according to their substrate specificities and the types of residues that participate in the aldol reaction and metal ion coordination. Phylogenetic tree (Fig. 1-2)

constructed for these aldolases showed the obvious differences between these subfamilies. In addition, aldolase existed widely in both eukaryote and prokaryote and were involved in glycolysis pathway [34].

1.4 asHPAL, a member of the HpaI/HpcH aldolase subfamily

4-Hydroxy-3-methyl-2-keto-pentanoate aldolase (asHPAL) is an aldolase from *Arthrobacter simplex* strain AKU 626 that belongs to the HpaI/HpcH aldolase subfamily of the class II aldolases. asHPAL uses Mg^{2+} as a prosthetic group to catalyze aldol reactions and has the potential for use in the synthesis of (2*S*,3*R*,4*S*)-4-hydroxyisoleucine (4-HIL) (Fig. 1-3) [35], which is a chiral amino acid extracted from the seeds of fenugreek *Trigonella foenum-graecum* [36]. Among the 8 possible enantiomers of 4-HIL, only (2*S*,3*R*,4*S*)-4-HIL exhibits the activity in enhancing the production of insulin from pancreatic β-cells [37-40]. Therefore, (2*S*,3*R*,4*S*)-4-HIL potentiates insulin secretion at supranormal glucose levels, whereas it is ineffective at low or basal glucose concentrations. The (2*S*,3*R*,4*S*)-4-HIL synthesis method using asHPAL involves two steps from the substrates 2-ketobutyrate and acetaldehyde (Fig. 1-3) [35]. In the first step, asHPAL catalyzes the aldol reaction between 2-ketobutyrate and acetaldehyde to form (3*S*,4*S*)-4-hydroxy-3-methyl-2-keto-pentanoate (HMKP). This product is converted to (2*S*,3*R*,4*S*)-4-HIL by branched-chain amino-acid aminotransferase (BCAT). The *S*-configuration of the C2 atom of (2*S*,3*R*,4*S*)-4-HIL is strictly controlled by BCAT [41, 42]. Therefore, the first step catalyzed by asHPAL is the key step in determining the spatial configuration of (2*S*,3*R*,4*S*)-4-HIL [35].

The HpaI/HpcH-aldolase subfamily is divided into three functional subgroups [15, 16]: 2,4-dihydroxyhept-2-ene-1,7-dioic acid (HHDE) aldolase, 2-keto-3-deoxyglucarate (KDG)

aldolase, and 4-hydroxy-2-oxovalerate (HKP) aldolase. YfaU (putative HHDE aldolase) [43] and YhaF (KDG aldolase) [44] from *Escherichia coli* and BphF (putative HKP-aldolase) from *Novosphingobium aromaticivorans* [45] were also used to examine whether they could stereoselectively catalyze the first step of the (2*S*,3*R*,4*S*)-4-HIL synthetic process similarly to asHPAL. The reaction was catalyzed by YfaU, YhaF, and BphF, but asHPAL exhibited the most preferential activity for the synthesis of (3*S*,4*S*)-HMKP (Fig. 1-4) [35]. Of the tested pH values, the stereoselectivity of asHPAL was highest at pH 6.0. However, the stereoselectivity is not strict for the production of (3*S*,4*S*)-HMKP. As described above, the stereoselective synthesis of (3*S*,4*S*)-HMKP is the key step of the designed (2*S*,3*R*,4*S*)-4-HIL biosynthetic process, which requires the uses of an enzyme with strict stereoselectivity. In addition, α-keto acids with several functional groups are potentially useful as intermediates for pharmaceutical synthesis. The enzymes with high stereoselectivity are expected to be useful for the stereoselective synthesis of other compounds.

Among the enzymes of the HpaI/HpcH-aldolase subfamily, 2,4-dihydroxyhept-2-ene- 1,7-dioic acid aldolase (HpcH) [46], YfaU [44], and YhaF [43] share 45%, 40%, and 38% sequence similarities to asHPAL, respectively. The catalytic mechanisms of HpcH, YfaU, and YhaF have been proposed based on their structures [43, 44, 46, 47]. Fig. 1-5 shows the proposed catalytic mechanism of YfaU in the reverse aldol reaction [47]. (a) The Mg^{2+}-bound water is activated to hydroxide ion by the intersubunit His49-Asp88 dyad. (b) The substrate, 4-hydroxy-2-oxopentanoate, binds to Mg^{2+} in a bidentate fashion with the C1 hydroxyl group and the C2 carbonyl oxygen. Arg74 interacts with the C2 carbonyl oxygen and the C4 hydroxyl group. An activated hydroxide ion abstracts the C4 hydroxyl proton, which is coupled with the breakage of the C3−C4 carbon−carbon bond to produce an aldehyde product and pyruvate enolate. (c) The C2 oxygen of pyruvate enolate is protonated by the Mg^{2+}-bound water. (d) The enzyme is returned to its ground state, and the catalytic cycle is completed by producing pyruvate and

acetaldehyde. In contrast, the aldol reaction of HpcH is thought to proceed inversely and is similar to that of YhaF (Fig. 1-6) [46]. (a) The Mg^{2+}-bound water is activated to hydroxide ion by His45. (b) The hydroxide ion abstracts a proton from the C2 methyl group of pyruvate to generate the nucleophilic enolate. (c) The enolate attacks the electrophilic carbon of the succinic semialdehyde acceptor. (d) The C4 oxygen is protonated by His45 to form a hydroxyl group. (e) The catalytic cycle is completed by producing 4-hydroxy-2-ketoheptane-1,7-dioate.

The sequence alignment of asHPAL with HpcH, YhaF, and YfaU shows that the proposed catalytic residues are conserved in asHPAL as His52, Arg77, and Asp91 (Fig. 1-7) [44, 47]. In addition, the Mg^{2+}-chelating residues of asHPAL are also conserved as Glu156 and Asp182. These correlations suggest that asHPAL works via a reaction mechanism similar to HpcH, YhaF, and YfaU. However, the sequence alignment cannot explain why asHPAL stereoselectively synthesizes (3*S*,4*S*)-HMKP. In addition, it remains unclear how asHPAL defines substrate specificity. asHPAL can catalyze the aldol reactions of small α-keto acids, including pyruvate and 2-ketoburyrate (Table 1-1). This selectivity also limits the utility of asHPAL for other stereoselective aldol reactions. The mechanistic bases of substrate specificities have not been reported for the other enzymes of the HpaI/HpcH-aldolase subfamily.

1.5 X-ray crystallography

X-ray crystallography is a powerful tool that is used to identify molecular structure at the atomic level. A beam of incident X-rays is diffracted into a number of different specific directions according to the distribution of the atoms in a crystal [48]. Each of the diffracted X-rays is detected as a diffraction spot by the detector. Measuring the distribution of the diffraction spots and subsequent data processing produce a three-dimensional diagram of the electron

density, which is useful for determining the mean positions of the atoms in the crystal. The protein structure of interest can be determined by using molecular replacement methods considering its amino acid sequence and the known structures of similar proteins [49]. From the structural information including the distance between atoms, we can understand the interaction between an enzyme and its substrate, the changes of protein states, and other structure-function relationships of proteins. In addition, structural results are often useful for protein engineering, such as to control protein function, expand substrate specificity, etc.

1.6 Purpose of the study

α-Keto acids are valuable intermediates that are conventionally used for pharmaceutical synthesis, and the aldol reaction is a useful tool to extend the carbon chain. asHPAL has potential as a biocatalyst for stereoselective aldol reactions, especially the stereoselective synthesis of (2*S*,3*R*,4*S*)-4-HIL coupled with the reaction of BCAT. The catalytic mechanisms of the HpaI/HpcH-aldolase subfamily toward α-keto acid substrates have been proposed in previous reports [43, 46, 47]. However, the mechanistic bases of the HpaI/HpcH-aldolase subfamily's stereoselectivity and substrate specificity remain unclear. Understanding these points will be conducive to improving the enzymatic properties of asHPAL. Here, I applied X-ray crystallography to reveal the structural basis of the stereoselectivity and substrate specificity of the aldol reaction catalyzed by asHPAL. Moreover, the obtained structural information was successfully used to improve the stereoselectivity and expand the substrate specificity of asHPAL.

Table 1-1 Substrate specificity of asHPAL.

α-Keto acid	Chemical formula	Availability[a]
Glyoxylate	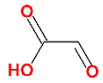	−
Pyruvate	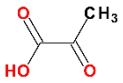	+
Hydroxypyruvate	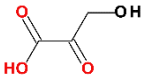	−
2-Ketobutyrate	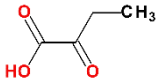	+
3-Methyl-2-ketobutyrate	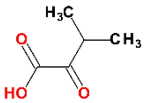	−
Oxalacetate	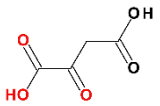	−
2-Ketopentanoate	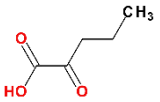	−
4-Methyl-2-oxovalerate	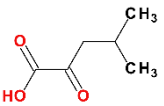	−
2-Ketoglutarate	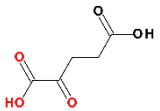	−
Phenylpyruvate	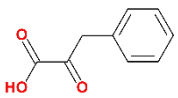	−

[a] "+" indicates that the compounds are used as substrates of asHPAL.

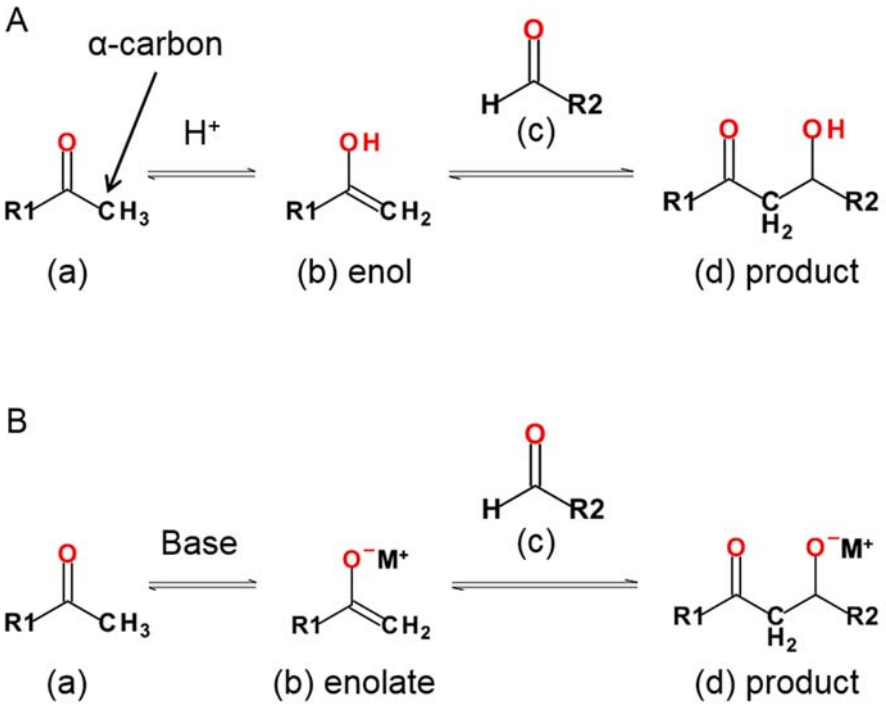

Fig. 1-1 Two different mechanisms of aldol reaction [15, 16].

(A) The pathway via an enol intermediate, in which carbonyl compound (a) is converted to enol (b) due to the nucleophilicity of α-carbon. The enol attacks aldehyde (c) to generate product (d).

(B) The pathway via an enolate intermediate, in which carbonyl compound (a) is deprotonated to form enolate (b). The enolate attacks the aldehyde (c) to generate product (d). "M^+" indicates a metal ion.

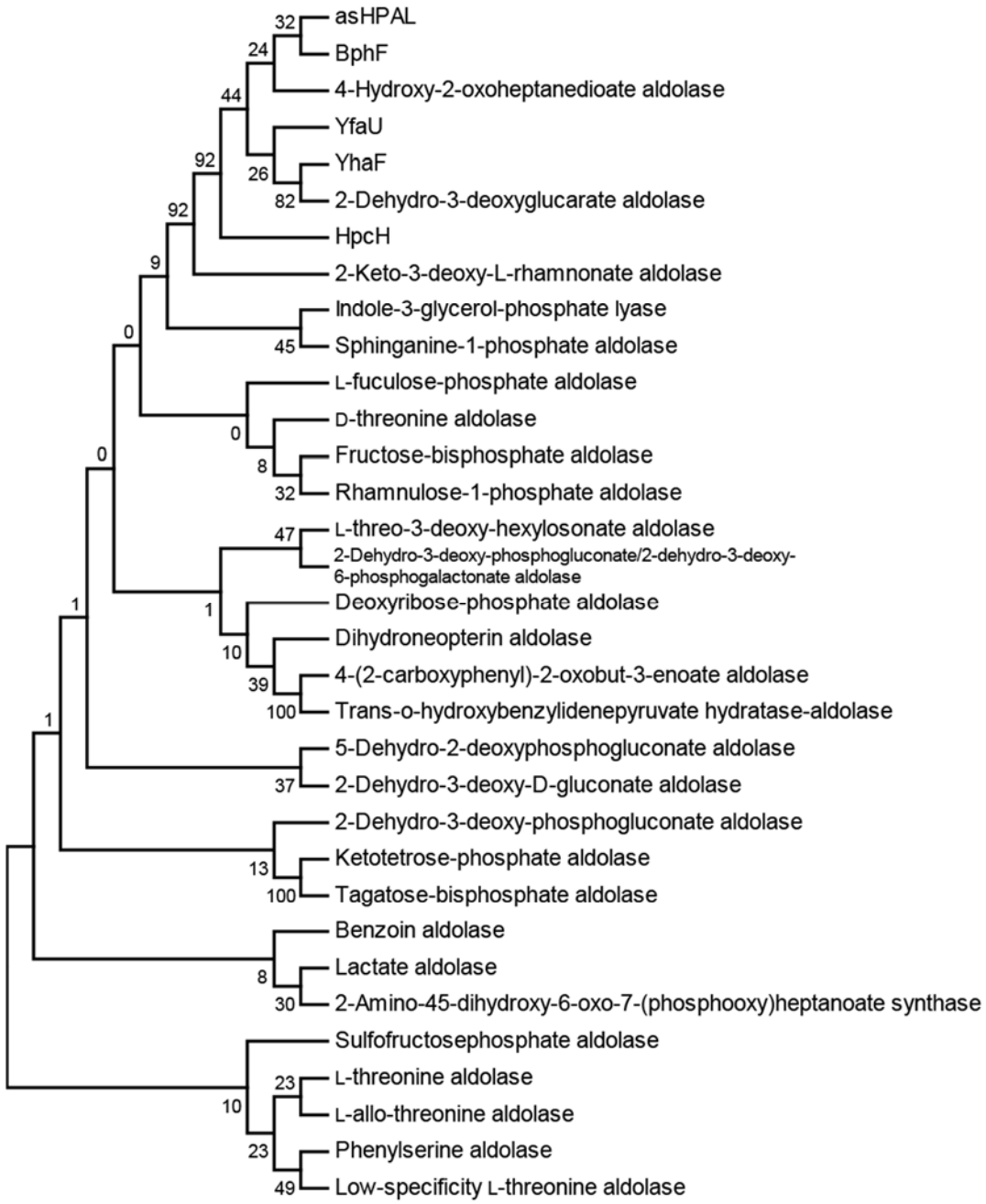

Fig. 1-2 Neighbor joining phylogenetic trees showing the relationship of asHPAL and other subfamilies of aldolase.

Similar results were obtained using maximum parsimony. The tree was constructed using the MEGA 6.0 program with the neighbor-joining algorithm[50]. Only bootstrap values greater than 50% are shown. The values are calculated with 0.2 substitution per amino acid site.

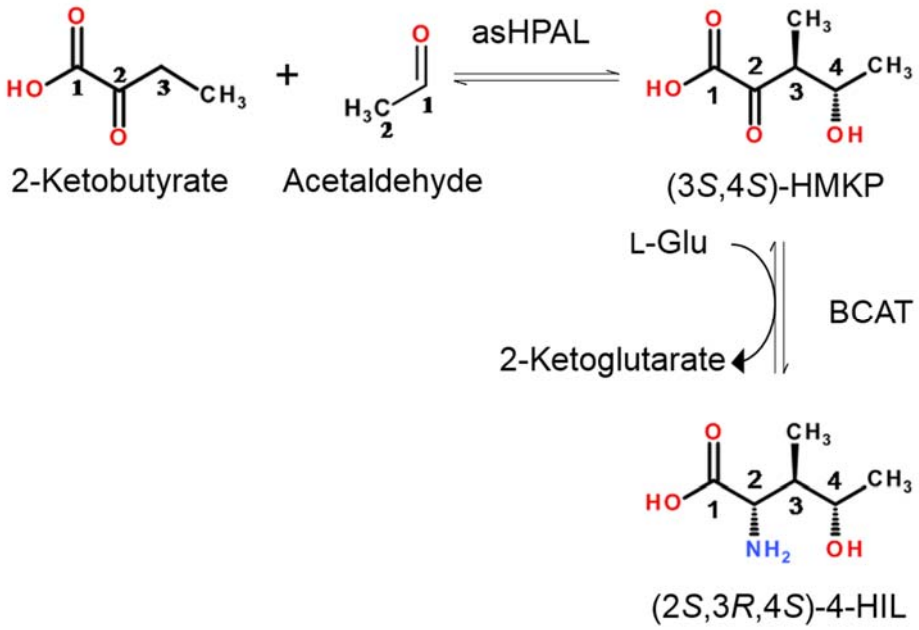

Fig. 1-3 Two-step enzymatic synthesis of (2*S*,3*R*,4*S*)-4-hydroxyisoleucine (HIL) by asHPAL and BCAT [35].

Firstly, asHPAL converts 2-ketobutyrate and acetaldehyde to (3*S*,4*S*)-4-hydroxy- 3-methyl-2-keto-pentanoate (HMKP). Secondly, (3*S*,4*S*)-HMKP is converted to (2*S*,3*R*,4*S*)-4-HIL by BCAT. In the second reaction, the amino group of L-glutamic acid (L-Glu) is transferred to (3*S*,4*S*)-HMKP.

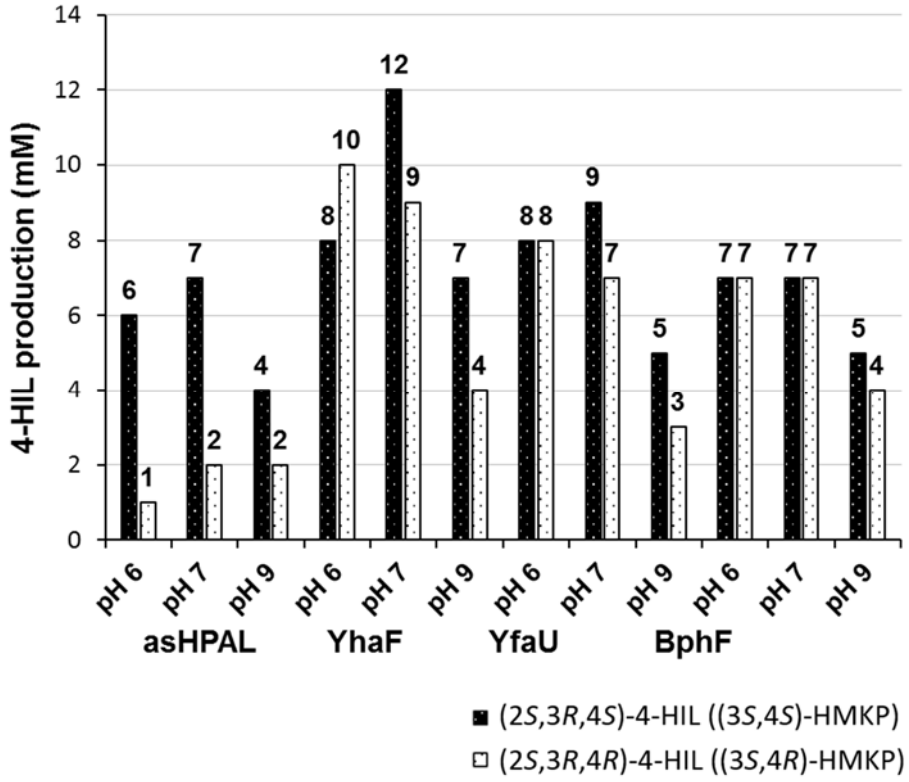

Fig. 1-4 pH dependency of 4-HIL enantiomer production catalyzed by each enzyme of the HpaI/HpcH-aldolase subfamily and BCAT.

The amounts of (2*S*,3*R*,4*S*)-4-HIL and (2*S*,3*R*,4*R*)-4-HIL are equivalently estimated as the amounts of (3*S*,4*S*)-HMKP and (3*S*,4*R*)-HMKP, respectively. The *S*-configuration of the C2 atom of 4-HIL is strictly controlled by the BCAT [41, 42]. In the sequential reaction to 4-HIL from 2-ketobutyrate and acetaldehyde (Fig. 1-2), the first reaction are catalyzed by each enzyme of the HpaI/HpcH-aldolase subfamily (asHPAL, YhaF, YfaU and BphF). asHPAL can preferentially catalyze the synthesis of (3*S*,4*S*)-HMKP [(2*S*,3*R*,4*S*)-4-HIL] [51].

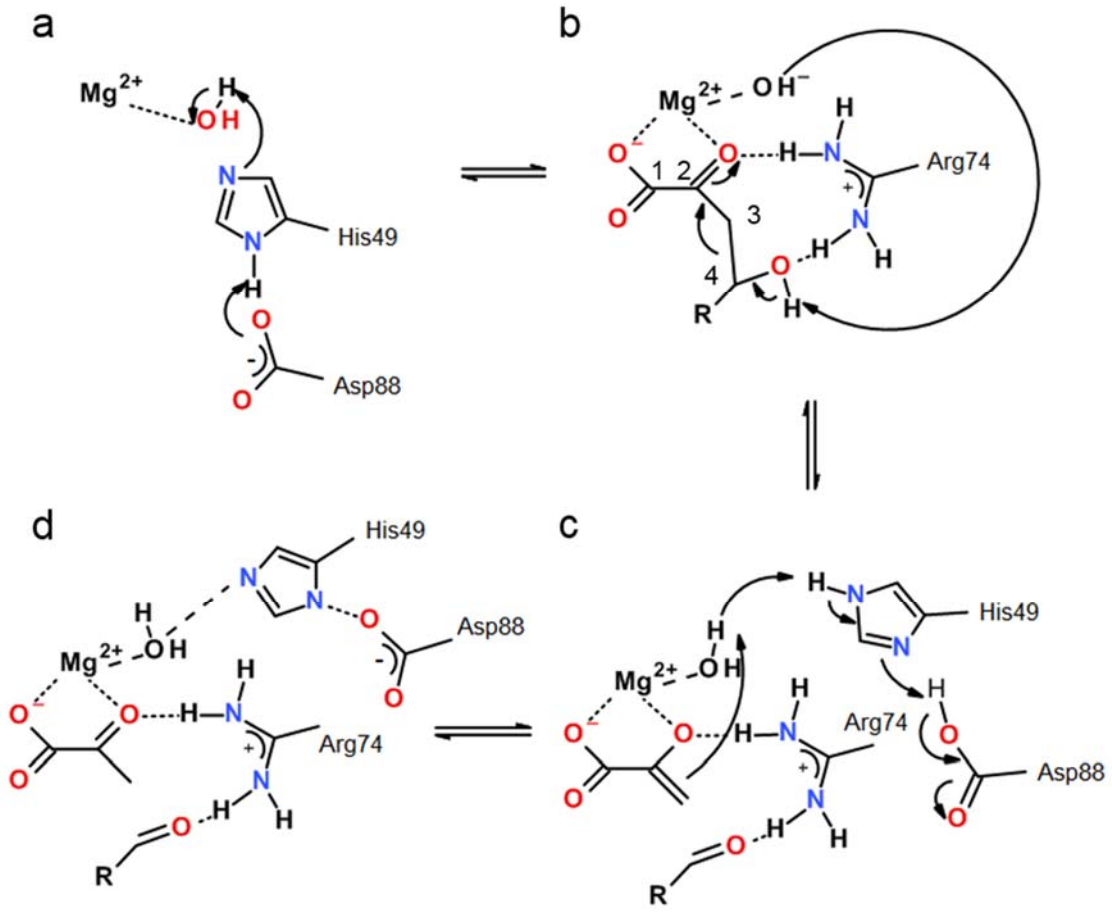

Fig. 1-5 Proposed catalytic mechanism of YfaU which catalyzes the decomposition of 2-keto-3-deoxy acid sugar.

(a) The Mg^{2+}-bound water is activated to hydroxide ion by the intersubunit His49-Asp88 dyad. (b) The substrate, 2-keto-3-deoxy acid sugar, binds to Mg^{2+} in a bidentate fashion with the C1 hydroxyl group and the C2 carbonyl oxygen. Arg74 interacts with the C2 carbonyl oxygen and the C4 hydroxyl group. An activated hydroxide ion abstracts the C4 hydroxyl proton, which is coupled with the breakage of the C3−C4 carbon−carbon bond to produce aldehyde product and pyruvate enolate. (c) The C2 oxygen of pyruvate enolate is protonated by the Mg^{2+}-bound water. (d) The enzyme is returned to its ground state, and the catalytic cycle is completed by producing pyruvate and acetaldehyde. [47].

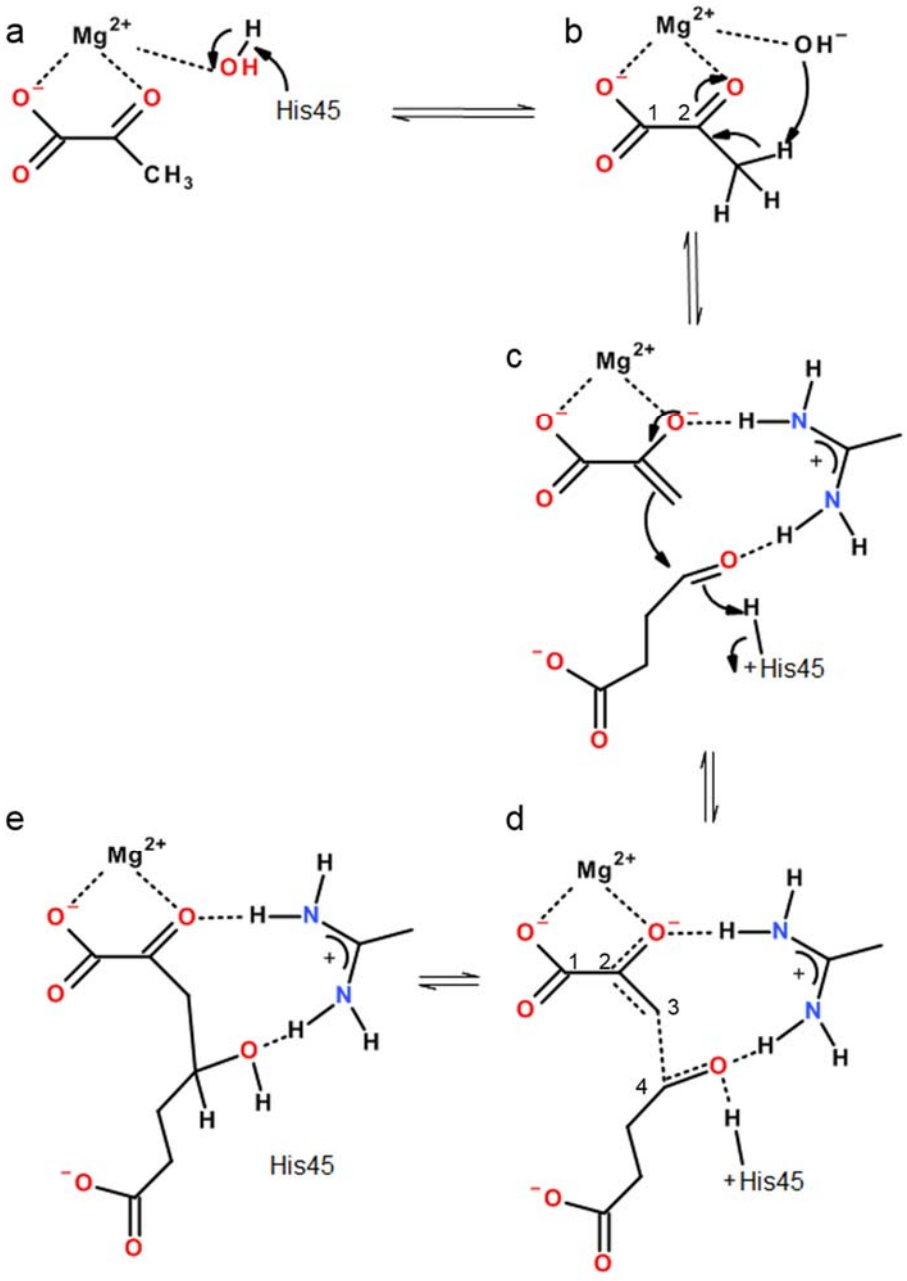

Fig. 1-6 The catalytic mechanism of HpcH which catalyzes aldol reaction.

(a) The Mg^{2+}-bound water is activated by a hydroxide ion from His45. (b) The hydroxide ion abstracts a proton from the C2 methyl group of pyruvate to generate the nucleophilic enolate. (c) The nucleophilic enolate attacks the electrophilic carbon of the succinic semialdehyde acceptor. (d) The C4 oxygen is protonated by His45 to form a hydroxyl group. (e) The enzyme adopts a ground state, and catalytic cycle is completed by producing 4-hydroxy-2-ketoheptane-1,7-dioate [46].

Fig. 1-7 Sequence alignment of asHPAL with other class II aldolases.

The amino acid sequence of asHPAL is aligned with those of other enzymes of HpaI/HpcH-aldolase subfamily, HpcH (45% sequence identity to asHPAL), YhaF (38%), YfaU (40%), and BphF (39%). The sequence alignment was generated by ClustalW [52]. Identical and highly conserved residues are indicated with asterisks, and double or single dots, respectively. Active-site residues are shown by red triangles. These enzymes share the amino acid residues which are important for the catalytic reaction.

Chapter 2

Crystal structure of asHPAL

2.1 Exordium

X-ray crystallography is a powerful technique for analyzing enzymatic mechanisms. This technique has been used to understand the structural bases of the stereoselectivity and substrate specificity of asHPAL.

High quality crystals, which diffract X-rays at high resolution, provide detailed structural information including the catalytic mechanism of enzymatic reactions. The discovery and optimization of appropriate crystallization conditions are the bottlenecks of X-ray crystallography. In addition, a large amount of protein (> 10 mg) of high purity is often required for crystallization experiments. Therefore, protein expression and purification are also important steps in X-ray crystallography, and the fundamental asHPAL preparation procedure is the basis of further biochemical analyses. In this chapter, I describe the protein preparation, crystallization, and X-ray diffraction data collection and processing used to determine the crystal structure of asHPAL. The purified protein was also used to evaluate the properties of asHPAL such as enzymatic activity and oligomer formation in solution.

2.2 Materials and methods

2.2.1 Materials

An *E. coli* plasmid vector for the expression of recombinant asHPAL and purified (2*S*,3*R*,4*S*)-4-HIL were provided by Prof. Dr. OGAWA Jun (Kyoto University). All other chemicals were of biochemical research grade and were purchased from Nacalai Tesque, Sigma-Aldrich, Wako Pure Chemical Industries, Hampton Research, Merck, and Tokyo Chemical Industry.

2.2.2 Protein expression

asHPAL was overexpressed in *E. coli* Rosetta (DE3) (Novagen) harboring the plasmid vector for recombinant asHPAL. The expressed protein (residues 1–259) has an N-terminal sequence including a His-tag. The *E. coli* cells were cultivated in Luria-Bertani (LB) medium (Merck) containing 30 μg ml^{-1} ampicillin at 310 K. The expression conditions for asHPAL were optimized by changing the induction temperature (291 K, 298 K, and 310 K) and the concentration of isopropyl β-D-thiogalactopyranoside (IPTG) (0.1 mM, 0.25 mM, 0.5 mM, and 1.0 mM final concentrations). Cell lysates were separated into soluble and insoluble fractions by centrifugation and then analyzed by sodium dodecyl sulfate-polyacrylamide gel electrophoresis (SDS-PAGE; total acrylamide concentration of the separation gel, 15%). The separation gel was stained with Coomassie Brilliant Blue (CBB) R-250. The optimal expression conditions were chosen based on the amount of asHPAL in the soluble fraction.

2.2.3 Purification of recombinant asHPAL

The harvested cells were suspended in buffer A (40 mM Tris-HCl, pH 7.5, 400 mM NaCl,

5 mM imidazole, and 1 mM DTT) and were then disrupted by sonication on ice. After centrifugation at 40,000 ×*g* at 277 K for 30 min, the supernatant was loaded onto a Ni-Sepharose 6 Fast Flow (GE Healthcare Life Sciences) column (3-ml gel bed) at 298 K. After washing with buffer B (40 mM Tris-HCl, pH 7.5, 400 mM NaCl, 50 mM imidazole, and 1 mM DTT), the asHPAL protein was eluted with buffer C (40 mM Tris-HCl, pH 7.5, 400 mM NaCl, 200 mM imidazole, and 1 mM DTT) at 298 K. The eluted protein was dialyzed against a 100-fold excess of the external solution (40 mM Tris-HCl, pH 7.5 and 1 mM DTT) at 277 K for 12 h.

The protein was further purified by anion-exchange column chromatography using the ÄKTA purifier system (GE Healthcare). The proteins were loaded onto a Resource Q 6-ml (GE Healthcare) column pre-equilibrated with 40 mM Tris-HCl (pH 7.5) at 277 K and were eluted with a linear gradient of 0–1 M NaCl in 40 mM Tris-HCl (pH 7.5) at 277 K. The purity of asHPAL was evaluated by SDS-PAGE (total acrylamide concentration of the separation gel, 15%). The separation gel was stained with CBB R-250. The purified asHPAL was dialyzed against 20 mM Tris-HCl (pH 7.5) at 277 K and was concentrated to 10 mg ml^{-1} using a Vivaspin 20 concentrator (molecular weight cut off, 5 k, hydrozart membrane; Vivascience) at 277 K. Protein concentrations were determined by the absorbance at 280 nm with a molar extinction coefficient of 14,565 M^{-1} cm^{-1} [53] and a molecular weight of 27,130.

2.2.4 Size-exclusion chromatography

本項の内容は、学術雑誌論文として出版する計画があるため公表できない。5 年以内に出版予定。

2.2.5 Assay for the stereoselectivity of asHPAL

本項の内容は、学術雑誌論文として出版する計画があるため公表できない。5 年

以内に出版予定。

2.2.6 Crystallization of asHPAL

The purified asHPAL (10 mg ml^{-1}) was used for crystallization experiments. Initial crystallization trials were performed by the sitting-drop vapor diffusion method using sparse-matrix screening kits: Crystal Screen HT, Index HT (Hampton Research), and Wizard I and II (Emerald Biosystems). Each drop was prepared by mixing equal volumes (0.7 μl) of the protein solution and a reservoir solution and was then equilibrated against 70 μl of the reservoir solution at 277 or 293 K.

After obtaining crystals, the 2D grid optimization of crystallization conditions (pH vs. precipitant concentration) was performed by the sitting-drop vapor diffusion method using 24-well Cryschem plates (Hampton Research). Each drop was prepared by mixing equal volumes (2.0 μl) of the protein solution and a reservoir solution and was then equilibrated against 400 μl of the reservoir solution at 293 K.

2.2.7 Data collection and processing

Each asHPAL crystal was picked up in a nylon loop (Hampton Research) and then transferred to a cryoprotectant solution prepared by mixing 76% (v/v) of the reservoir solution and 24% (v/v) of glycerol. The crystals were mounted on the X-ray diffractometers and were flash-cooled in a cryo-nitrogen stream (95 K). The X-ray diffraction data set (600 images) of an asHPAL crystal grown at pH 7.7 was collected with synchrotron radiation and an ADSC Quantum 210 detector on BL-5A beamline at Photon Factory (Ibaraki, Japan). The parameters of data collection were as follows: wavelength, 1.0000 Å; collection angle, 180°; oscillation angle, 0.3°; crystal-to-detector distance, 142 mm; and exposure time, 0.5 sec.

2.2.8 Structure determination and model refinement

本項の内容は、学術雑誌論文として出版する計画があるため公表できない。5 年以内に出版予定。

2.3 Results and discussion

2.3.1 Expression and purification of asHPAL

After optimizing expression conditions, asHPAL expression was induced by the addition of IPTG to a final concentration of 0.5 mM when the optimal density at 600 nm reached 0.6, and the cells were then cultivated at 293 K for 16 h. The cultivated cells were harvested by centrifugation at 5,000 ×*g* at 277 K for 20 min. The cell pellets were rapidly frozen in liquid nitrogen and stored at 193 K.

Soluble and insoluble fractions were separated by centrifugation after cell lysis. The supernatant was loaded onto a Ni-Sepharose 6 Fast Flow (GE Healthcare) column. The eluate was analyzed by SDS-PAGE (Fig. 2-2). The results showed that the eluate contained abundant asHPAL and small amounts of other proteins. Further purification was performed by anion-exchange chromatography to remove the contaminants. A major peak was observed in the resulting chromatogram at the NaCl concentration of 42% (Fig. 2-3A). The three fractions comprising the major peak were assessed by SDS-PAGE (Fig. 2-3B). The results showed that the major peak primarily contained asHPAL; however, small amounts of other proteins remained in the major peak. According to the shape of the major peak, the purified asHPAL was not electrostatically heterogeneous, but the small peak appeared to overlap with the major peak. The first two fractions were chosen to avoid the small peak and were used for crystallization and other assays. After concentration, the yield of soluble asHPAL was 15 mg per one liter of *E. coli* culture.

2.3.2 Oligomeric state of asHPAL

本項の内容は、学術雑誌論文として出版する計画があるため公表できない。5 年

以内に出版予定。

2.3.3 Stereoselective activity of purified asHPAL

本項の内容は、学術雑誌論文として出版する計画があるため公表できない。5 年以内に出版予定。

2.3.4 Crystallization of asHPAL

asHPAL crystals were obtained with the reservoir solution containing 100 mM HEPES (pH 7.5), 30% (v/v) PEG 400, and 200 mM $MgCl_2$ at 293 K. After 2D grid optimization of crystallization conditions, the best crystals of asHPAL were reproducibly obtained with the reservoir solution containing 100 mM HEPES-Na (pH 7.7), 30% (v/v) PEG 400, and 200 mM $MgCl_2$ at 293 K (Fig. 2-10) for 1 day.

2.3.5 Data collection and structure determination

本項の内容は、学術雑誌論文として出版する計画があるため公表できない。5 年以内に出版予定。

2.3.6 Overall structure of asHPAL

本項の内容は、学術雑誌論文として出版する計画があるため公表できない。5 年以内に出版予定。

2.3.7 Structural comparison of asHPAL with the other enzymes of the HpaI/HpcH-aldolase subfamily

本項の内容は、学術雑誌論文として出版する計画があるため公表できない。5 年以内に出版予定。

2.4 Conclusion

本項の内容は、学術雑誌論文として出版する計画があるため公表できない。5 年以内に出版予定。

Chapter 3

Structural basis for the stereoselective aldol reaction of asHPAL

本章の内容は、学術雑誌論文として出版する計画があるため公表できない。5年以内に出版予定。

Chapter 4

Mechanism of substrate specificity of asHPAL

本章の内容は、学術雑誌論文として出版する計画があるため公表できない。5 年以内に出版予定。

Chapter 5

General discussion

本章の内容は、学術雑誌論文として出版する計画があるため公表できない。5 年以内に出版予定。

References

[1] Wade, L.G., *Organic chemistry*. 1999, Upper Saddle River, N.J.: Prentice Hall.

[2] Anonymous, Annual Report in Medicinal Chemistry, 1992-2009, 2009. **27-44**.

[3] Bartholow, M., *Top 200 Drugs of 2010.* Pharmacy Times, 2010.

[4] Nelson, D.L., D.L. Nelson, A.L. Lehninger, and M.M. Cox, *Lehninger principles of biochemistry*. 2008, New York: W.H. Freeman.

[5] Leffingwell, J.C., *Chirality & Bioactivity I.: Pharmacology.* Leffingwell Reports, 2003. **3**: p. 1-27.

[6] Blaschke, G., *Chromatographische Racemattrennung von Thalidomid und teratogene Wirkung der Enantiomere.* Arzneimittelforschung, 1979. **29**: p. 1640-1642.

[7] Nguyen, L.A., H. He, and C. Pham-Huy, *Chiral Drugs: An Overview.* International Journal of Biomedical Science : IJBS, 2006. **2**(2): p. 85-100.

[8] McNaught, A.D., A. Wilkinson, A.D. Jenkins, P. International Union of, and C. Applied, *IUPAC compendium of chemical terminology the gold book*. 2006, [Research Triangle Park, N.C.]: International Union of Pure and Applied Chemistry.

[9] Bauer, E.B., *Chiral-at-metal complexes and their catalytic applications in organic synthesis.* Chemical Society Reviews, 2012. **41**(8): p. 3153-3167.

[10] Heitbaum, M., F. Glorius, and I. Escher, *Asymmetric Heterogeneous Catalysis.* Angewandte Chemie International Edition, 2006. **45**(29): p. 4732-4762.

[11] Roos, G., *Compendium of chiral auxiliary applications*. 2002, San Diego: Academic Press.

[12] Faber, K., *Biotransformations in organic chemistry : a textbook*. 2004, Berlin [etc.]: Springer.

[13] Mukaiyama, T., *The Directed Aldol Reaction*, in *Organic Reactions*. 2004, John Wiley & Sons, Inc.

[14] Smith, M., J. March, and J. March, *March's advanced organic chemistry : reactions,*

mechanisms, and structure. 2001, New York: Wiley.

[15] *Modern aldol reactions 1, 1*. 2004, Weinheim: Wiley-VCH.

[16] *Modern aldol reactions 2, 2*. 2004, Weinheim: Wiley-VCH.

[17] Wurtz, A., *Ueber einen Aldehyd-Alkohol.* Journal für Praktische Chemie, 1872. **5**(1): p. 457-464.

[18] Mestres, R., *A green look at the aldol reaction.* Green Chemistry, 2004. **6**(12): p. 583-603.

[19] Braun, M. and R. Devant, *(R)- and (S)-2-acetoxy-1,1,2-triphenylethanol - effective synthetic equivalents of a chiral acetate enolate.* Tetrahedron Letters, 1984. **25**(44): p. 5031-5034.

[20] Brown, H.C., R.K. Dhar, R.K. Bakshi, P.K. Pandiarajan, and B. Singaram, *Major effect of the leaving group in dialkylboron chlorides and triflates in controlling the stereospecific conversion of ketones into either [E]- or [Z]-enol borinates.* Journal of the American Chemical Society, 1989. **111**(9): p. 3441-3442.

[21] Ireland, R.E. and A.K. Willard, *The stereoselective generation of ester enolates.* Tetrahedron Letters, 1975. **16**(46): p. 3975-3978.

[22] Narula, A.S., *An analysis of the diastereomeric transition state interactions for the kinetic deprotonation of acyclic carbonyl derivatives with lithium diisopropylamide.* Tetrahedron Letters, 1981. **22**(41): p. 4119-4122.

[23] Ireland, R.E., P. Wipf, and J.D. Armstrong, *Stereochemical control in the ester enolate Claisen rearrangement. 1. Stereoselectivity in silyl ketene acetal formation.* The Journal of Organic Chemistry, 1991. **56**(2): p. 650-657.

[24] Xie, L., K.M. Isenberger, G. Held, and L.M. Dahl, *Highly Stereoselective Kinetic Enolate Formation: Steric vs Electronic Effects.* J Org Chem, 1997. **62**(21): p. 7516-7519.

[25] Evans, D.A., J.V. Nelson, E. Vogel, and T.R. Taber, *Stereoselective aldol condensations*

via boron enolates. Journal of the American Chemical Society, 1981. **103**(11): p. 3099-3111.

[26] Roush, W.R., *Concerning the diastereofacial selectivity of the aldol reactions of .alpha.-methyl chiral aldehydes and lithium and boron propionate enolates.* The Journal of Organic Chemistry, 1991. **56**(13): p. 4151-4157.

[27] Boyer, P.D., E.G. Krebs, and D.S. Sigman, *The Enzymes*. 1970: Academic Press.

[28] Fessner, W.-D., A. Schneider, H. Held, G. Sinerius, C. Walter, M. Hixon, and J.V. Schloss, *The Mechanism of Class II, Metal-Dependent Aldolases.* Angewandte Chemie International Edition in English, 1996. **35**(19): p. 2219-2221.

[29] Dreyer, M.K. and G.E. Schulz, *Catalytic Mechanism of the Metal-dependent Fuculose Aldolase fromEscherichia colias Derived from the Structure.* Journal of Molecular Biology, 1996. **259**(3): p. 458-466.

[30] Lorentzen, E., B. Siebers, R. Hensel, and E. Pohl, *Mechanism of the Schiff Base Forming Fructose-1,6-bisphosphate Aldolase: Structural Analysis of Reaction Intermediates‡.* Biochemistry, 2005. **44**(11): p. 4222-4229.

[31] Horecker, B.L., P.T. Rowley, E. Grazi, T. Cheng, and O. Tchola, *THE MECHANISM OF ACTION OF ALDOLASES. IV. LYSINE AS THE SUBSTRATE-BINDING SITE.* Biochem Z, 1963. **338**: p. 36-51.

[32] St-Jean, M. and J. Sygusch, *Stereospecific proton transfer by a mobile catalyst in mammalian fructose-1,6-bisphosphate aldolase.* J Biol Chem, 2007. **282**(42): p. 31028-37.

[33] Rutter, W.J., *EVOLUTION OF ALDOLASE.* Fed Proc, 1964. **23**: p. 1248-57.

[34] Liapounova, N.A., V. Hampl, P.M.K. Gordon, C.W. Sensen, L. Gedamu, and J.B. Dacks, *Reconstructing the Mosaic Glycolytic Pathway of the Anaerobic Eukaryote Monocercomonoides.* Eukaryotic Cell, 2006. **5**(12): p. 2138-2146.

[35] Ogawa, J., H. Yamanaka, J. Mano, Y. Doi, N. Horinouchi, T. Kodera, N. Nio, S.V. Smirnov, N.N. Samsonova, Y.I. Kozlov, and S. Shimizu, *Synthesis of 4-hydroxyisoleucine by the aldolase-transaminase coupling reaction and basic characterization of the aldolase from Arthrobacter simplex AKU 626.* Biosci Biotechnol Biochem, 2007. **71**(7): p. 1607-15.

[36] Fowden, L., H.M. Pratt, and A. Smith, *4-Hydroxyisoleucine from Seed of Trigonella-Foenum-Graecum.* Phytochemistry, 1973. **12**(7): p. 1707-1711.

[37] Gieren, A., Narayana.P, W. Hoppe, M. Hasan, K. Michl, T. Wieland, H.O. Smith, G. Jung, and Breitmai.E, *Components of Green Deathcap Toadstool, Amanita-Phalloides .44. Configuration of Hydroxylated Isoleucines from Amatoxins.* Annalen Der Chemie-Justus Liebig, 1974(10): p. 1561-1569.

[38] Alcock, N.W., D.H.G. Crout, M.V.M. Gregorio, E. Lee, G. Pike, and C.J. Samuel, *Stereochemistry of the 4-hydroxyisoleucine from Trigonella foenum-graecum.* Phytochemistry, 1989. **28**(7): p. 1835-1841.

[39] Jacob, M., M.L. Roumestant, P. Viallefont, and J. Martinez, *Enantioselective synthesis of gamma-hydroxynorvaline.* Synlett, 1997(6): p. 691-692.

[40] Broca, C., M. Manteghetti, R. Gross, Y. Baissac, M. Jacob, P. Petit, Y. Sauvaire, and G. Ribes, *4-Hydroxyisoleucine: effects of synthetic and natural analogues on insulin secretion.* Eur J Pharmacol, 2000. **390**(3): p. 339-45.

[41] Mamer, O.A. and M.L. Reimer, *On the mechanisms of the formation of L-alloisoleucine and the 2-hydroxy-3-methylvaleric acid stereoisomers from L-isoleucine in maple syrup urine disease patients and in normal humans.* J Biol Chem, 1992. **267**(31): p. 22141-7.

[42] Hall, T.R., R. Wallin, G.D. Reinhart, and S.M. Hutson, *Branched chain aminotransferase isoenzymes. Purification and characterization of the rat brain isoenzyme.* Journal of Biological Chemistry, 1993. **268**(5): p. 3092-3098.

[43] Wright, A., A. Blewett, V. Fulop, R. Cooper, S. Burrows, C. Jones, and D. Roper, *Expression, purification, crystallization and preliminary characterization of an HHED aldolase homologue from Escherichia coli K12.* Acta Crystallogr D Biol Crystallogr, 2002. **58**(Pt 12): p. 2191-3.

[44] Izard, T. and N.C. Blackwell, *Crystal structures of the metal-dependent 2-dehydro-3-deoxy-galactarate aldolase suggest a novel reaction mechanism.* EMBO J, 2000. **19**(15): p. 3849-56.

[45] Romine, M.F., L.C. Stillwell, K.K. Wong, S.J. Thurston, E.C. Sisk, C. Sensen, T. Gaasterland, J.K. Fredrickson, and J.D. Saffer, *Complete sequence of a 184-kilobase catabolic plasmid from Sphingomonas aromaticivorans F199.* J Bacteriol, 1999. **181**(5): p. 1585-602.

[46] Rea, D., V. Fulop, T.D. Bugg, and D.I. Roper, *Structure and mechanism of HpcH: a metal ion dependent class II aldolase from the homoprotocatechuate degradation pathway of Escherichia coli.* J Mol Biol, 2007. **373**(4): p. 866-76.

[47] Rea, D., R. Hovington, J.F. Rakus, J.A. Gerlt, V. Fulop, T.D. Bugg, and D.I. Roper, *Crystal structure and functional assignment of YfaU, a metal ion dependent class II aldolase from Escherichia coli K12.* Biochemistry, 2008. **47**(38): p. 9955-65.

[48] Donnay, J.D.H., *X-Ray Crystallographic Technology. André Guinier; trans. by T. L. Tippell; Kathleen Lonsdale, Ed. London: Hilger and Watts, 1952. (U.S. distrib.: Jarrell-Ash, Boston.) 330 pp. Illus. + plates. $9.50.* Science, 1953. **118**(3077): p. 757-758.

[49] Ealick, S., *Principles of protein X-ray crystallography by J. Drenth.* Acta Crystallographica Section D, 1995. **51**(2): p. 248.

[50] Tamura, K., G. Stecher, D. Peterson, A. Filipski, and S. Kumar, *MEGA6: Molecular Evolutionary Genetics Analysis version 6.0.* Molecular Biology and Evolution, 2013.

[51] Smirnov, S.V., N.N. Samsonova, A.E. Novikova, N.G. Matrosov, N.Y. Rushkevich, T.

Kodera, J. Ogawa, H. Yamanaka, and S. Shimizu, *A novel strategy for enzymatic synthesis of 4-hydroxyisoleucine: identification of an enzyme possessing HMKP (4-hydroxy-3-methyl-2-keto-pentanoate) aldolase activity.* FEMS Microbiol Lett, 2007. **273**(1): p. 70-7.

[52] Larkin, M.A., G. Blackshields, N.P. Brown, R. Chenna, P.A. McGettigan, H. McWilliam, F. Valentin, I.M. Wallace, A. Wilm, R. Lopez, J.D. Thompson, T.J. Gibson, and D.G. Higgins, *Clustal W and Clustal X version 2.0.* Bioinformatics, 2007. **23**(21): p. 2947-2948.

[53] Pace, C.N., F. Vajdos, L. Fee, G. Grimsley, and T. Gray, *How to measure and predict the molar absorption coefficient of a protein.* Protein Sci, 1995. **4**(11): p. 2411-23.

[54] Kinoshita, T., Y. Kasahara, and N. Nimura, *Reversed-phase high-performance liquid chromatographic resolution of non-esterified enantiomeric amino acids by derivatization with 2,3,4,6-tetra-o-acetyl-β-d-glucopyranosyl isothiocyanate and 2,3,4-tri-o-acetyl-α-d-arabinopyranosyl isothiocyanate.* Journal of Chromatography A, 1981. **210**(1): p. 77-81.

[55] Collaborative Computational Project, N., *The CCP4 suite: programs for protein crystallography.* Acta Crystallogr D Biol Crystallogr, 1994. **50**(Pt 5): p. 760-3.

[56] Vagin, A. and A. Teplyakov, *MOLREP: an Automated Program for Molecular Replacement.* Journal of Applied Crystallography, 1997. **30**(6): p. 1022-1025.

[57] Cohen, S.X., M. Ben Jelloul, F. Long, A. Vagin, P. Knipscheer, J. Lebbink, T.K. Sixma, V.S. Lamzin, G.N. Murshudov, and A. Perrakis, *ARP/wARP and molecular replacement: the next generation.* Acta Crystallogr D Biol Crystallogr, 2008. **64**(Pt 1): p. 49-60.

[58] Emsley, P. and K. Cowtan, *Coot: model-building tools for molecular graphics.* Acta Crystallogr D Biol Crystallogr, 2004. **60**(Pt 12 Pt 1): p. 2126-32.

[59] Vagin, A.A., R.A. Steiner, A.A. Lebedev, L. Potterton, S. McNicholas, F. Long, and G.N. Murshudov, *REFMAC5 dictionary: organization of prior chemical knowledge and*

guidelines for its use. Acta Crystallogr D Biol Crystallogr, 2004. **60**(Pt 12 Pt 1): p. 2184-95.

[60] Laskowski, R.A., M.W. MacArthur, D.S. Moss, and J.M. Thornton, *PROCHECK: a program to check the stereochemical quality of protein structures.* Journal of Applied Crystallography, 1993. **26**(2): p. 283-291.

[61] Holm, L. and P. Rosenstrom, *Dali server: conservation mapping in 3D.* Nucleic Acids Res, 2010. **38**(Web Server issue): p. W545-9.

[62] Hasegawa, H. and L. Holm, *Advances and pitfalls of protein structural alignment.* Curr Opin Struct Biol, 2009. **19**(3): p. 341-8.

[63] Andrews, P., *Estimation of the molecular weights of proteins by Sephadex gel-filtration.* Biochemical Journal, 1964. **91**(2): p. 222-233.

[64] Matthews, B.W., *Solvent content of protein crystals.* J Mol Biol, 1968. **33**(2): p. 491-7.

[65] Vella, F., *Introduction to protein structure. By C Branden and J Tooze. pp 302. garland publishing, New York. 1991 ISBN 0–8513–0270–3 (pbk).* Biochemical Education, 1992. **20**(2): p. 121-122.

[66] Kabsch, W., *Xds*. Acta Crystallogr D Biol Crystallogr, 2010. **66**(Pt 2): p. 125-32.

[67] Chemical Computing Group Inc., S.S.W., Suite #910, Montreal, QC, Canada, H3A 2R7, 2013. , *Molecular Operating Environment (MOE), 2013.08.*

[68] Edelsbrunner, H., M. Facello, F. Ping, and L. Jie. *Measuring proteins and voids in proteins*. in *System Sciences, 1995. Proceedings of the Twenty-Eighth Hawaii International Conference on*. 1995.

[69] Goto, J., R. Kataoka, H. Muta, and N. Hirayama, *ASEDock-docking based on alpha spheres and excluded volumes.* J Chem Inf Model, 2008. **48**(3): p. 583-90.

[70] 中村, 博., *パソコンによるFT-NMRのデータ処理* 第 2 版 ed. 2009: 三共出版. ix, 134p.

[71] Lineweaver, H. and D. Burk, *The Determination of Enzyme Dissociation Constants.*

Journal of the American Chemical Society, 1934. **56**(3): p. 658-666.

[72] Michaelis, L. and M.L. Menten, *{Die kinetik der invertinwirkung}*. Biochem. Z, 1913. **49**(333-369): p. 352.

[73] Cederstav, A.K. and B.M. Novak, *Investigations into the Chemistry of Thermodynamically Unstable Species. The Direct Polymerization of Vinyl Alcohol, the Enolic Tautomer of Acetaldehyde.* Journal of the American Chemical Society, 1994. **116**(9): p. 4073-4074.

[74] Otwinowski, Z. and W. Minor, *Processing of X-ray diffraction data collected in oscillation mode*. 1997, Elsevier. p. 307-326.

[75] Sutton, P.W., J.P. Adams, I. Archer, D. Auriol, M. Avi, C. Branneby, A.J. Collis, B. Dumas, T. Eckrich, I. Fotheringham, R. ter Halle, S. Hanlon, M. Hansen, K.E. Holt-Tiffin, R.M. Howard, G.W. Huisman, H. Iding, K. Kiewel, M. Kittelmann, E. Kupfer, K. Laumen, F. Lefèvre, S. Luetz, D.P. Mangan, V.A. Martin, H.-P. Meyer, T.S. Moody, A. Osorio-Lozada, K. Robins, R. Snajdrova, M.D. Truppo, A. Wells, B. Wirz, and J.W. Wong, *Biocatalysis in the Fine Chemical and Pharmaceutical Industries*, in *Practical Methods for Biocatalysis and Biotransformations 2*. 2012, John Wiley & Sons, Ltd. p. 1-59.

[76] Dale, J.A., D.L. Dull, and H.S. Mosher, *.alpha.-Methoxy-.alpha.-trifluoromethylphenylacetic acid, a versatile reagent for the determination of enantiomeric composition of alcohols and amines.* The Journal of Organic Chemistry, 1969. **34**(9): p. 2543-2549.

[77] Ohtani, I., T. Kusumi, Y. Kashman, and H. Kakisawa, *High-field FT NMR application of Mosher's method. The absolute configurations of marine terpenoids.* Journal of the American Chemical Society, 1991. **113**(11): p. 4092-4096.

[78] Hoye, T.R., C.S. Jeffrey, and F. Shao, *Mosher ester analysis for the determination of*

absolute configuration of stereogenic (chiral) carbinol carbons. Nat. Protocols, 2007. **2**(10): p. 2451-2458.

[79] Flack, H.D. and G. Bernardinelli, *The use of X-ray crystallography to determine absolute configuration.* Chirality, 2008. **20**(5): p. 681-90.

[80] Kobayashi, Y., N. Hayashi, and Y. Kishi, *Toward the creation of NMR databases in chiral solvents: bidentate chiral NMR solvents for assignment of the absolute configuration of acyclic secondary alcohols.* Org Lett, 2002. **4**(3): p. 411-4.

[81] Ghosh, I., H. Zeng, and Y. Kishi, *Application of chiral lanthanide shift reagents for assignment of absolute configuration of alcohols.* Org Lett, 2004. **6**(25): p. 4715-8.

[82] Kobayashi, Y., N. Hayashi, and Y. Kishi, *Application of chiral bidentate NMR solvents for assignment of the absolute configuration of alcohols: scope and limitation.* Tetrahedron Letters, 2003. **44**(40): p. 7489-7491.

[83] Freedman, T.B., X. Cao, R.K. Dukor, and L.A. Nafie, *Absolute configuration determination of chiral molecules in the solution state using vibrational circular dichroism.* Chirality, 2003. **15**(9): p. 743-58.

[84] Thompson, J.D., D.G. Higgins, and T.J. Gibson, *CLUSTAL W: improving the sensitivity of progressive multiple sequence alignment through sequence weighting, position-specific gap penalties and weight matrix choice.* Nucleic Acids Research, 1994. **22**(22): p. 4673-4680.

[85] Robert, X. and P. Gouet, *Deciphering key features in protein structures with the new ENDscript server.* Nucleic Acids Research, 2014. **42**(W1): p. W320-W324.

Acknowledgments

I would like to express the most sincere thanks to my supervisor, Prof. TANOKURA Masaru. He kept guiding me to the right path, offering valuable advice, keeping me inspired, and trying to build a research atmosphere as pleasant as possible. Without him, I could not have developed my knowledge and research skills so smoothly.

I deeply appreciate Prof. OGAWA Jun and Dr. HIBI Makoto at Kyoto University. The recombinant asHPAL expression plasmid and catalytic activities analysis method was provided by them. Most of the results described in this thesis would not have been obtained without collaboration with them.

I am also grateful to Dr. NAGATA Koji, Associate Professor in Tanokura's laboratory at the University of Tokyo. He always supports me to advance my research, and understands what the problem is.

I also want to thank Dr. OKAI Masahiko and Dr. MIYAKAWA Takuya, for teaching me how important it is to think about vents from a broad standpoint of view, as well as the skills of X-ray structural analysis. It is a pleasure to have worked with all the members of TANOKURA laboratory. They now constitute an important and indispensable dimension in my life.

I am extremely thankful to the staff of the Photon Factory of the National Laboratory for High Energy Physics and SPring-8 for their assistance.

Finally, I am deeply grateful to my family and friends for their constant help and the financial support from University of Tokyo that made my doctoral study possible.